Mn antisites and order-disorder transition in the $(MnBi_2Te_4)$ $(Bi_2Te_3)_n$ magnetic topological insulators

Ifeanyi John Onuorah

(University of Parma, Italy)

21st July, 2025

Outline

‣ Interplay of topology and magnetic order: Case of $MnBi_2Te_4$

‣ $MnBi_2Te_4$ a highly tunable material platform $\rightarrow$ the $(MnBi_2Te_4).(Bi_2Te_3)_n$ family

‣ Influence of native antisite intermixing on the magnetic behaviour of the $(MnBi_2Te_4).(Bi_2Te_3)_n$ family: Insights from:

   ✓ Bulk magnetometry measurements

   ✓ NMR

   ✓ µSR measurements

‣ Summary

Interplay of topology and magnetic order

Topological Insulator
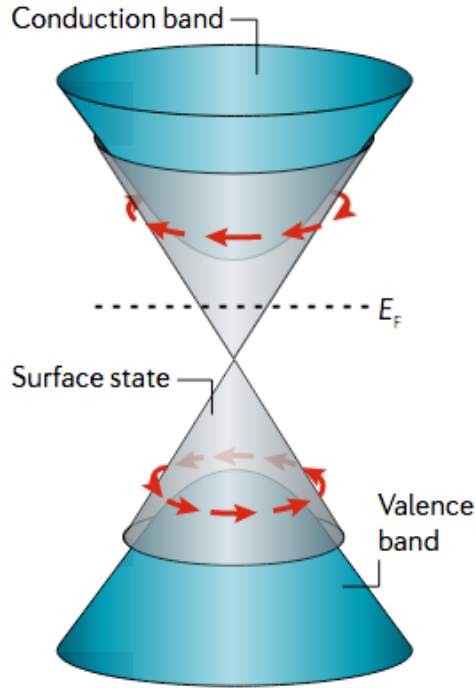
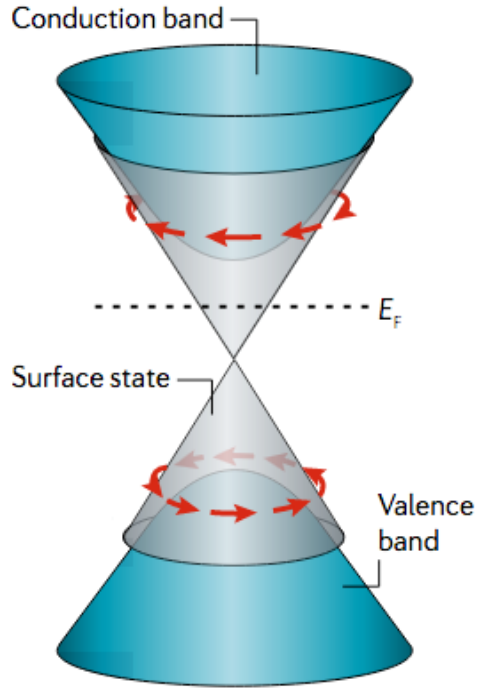## Magnetic topological Insulator
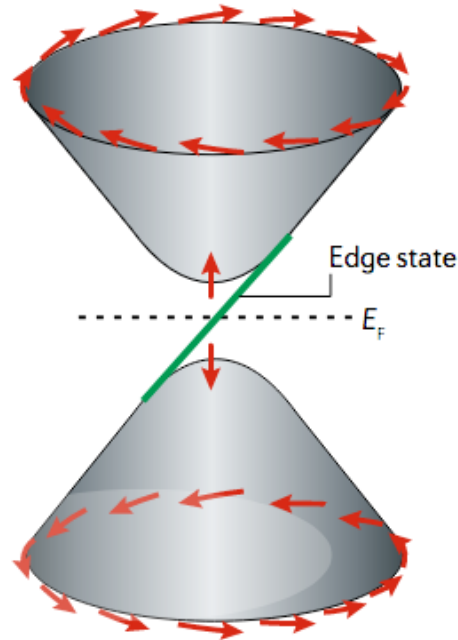
- ▸ Insulating bulk & conducting surface state

- ▸ Massless Dirac-like dispersion of the surface state

- ▸ Breaking time reversal symmetry in the presence of magnetism can open a gap in topological surface states

- ▸ Can enable versatile and tunable quantum phases including:

  - • High-order topological phases

  - • Axion electrodynamics
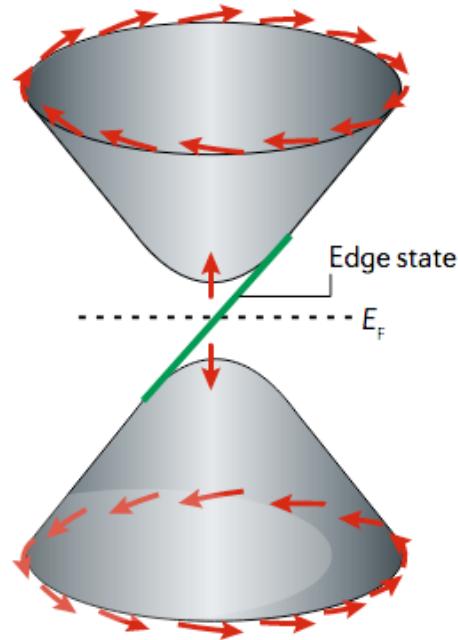
  - • Quantum anomalous Hall effect

Tokura Y. et al,, Nature review Physics 1, 126-143 (2019)

Interplay of topology and magnetic order

Topological Insulator

Magnetic topological Insulator

▸ Ordinarily realized by chemical doping of topological insulators with transition metal oxides

Conduction band

E_F

Surface state
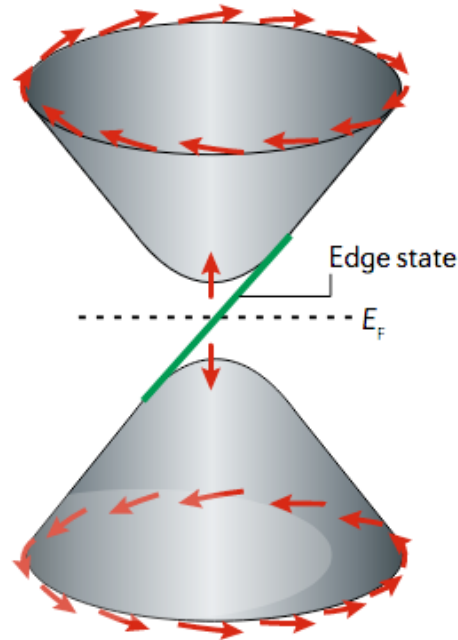
Valence band

Edge state

E_F

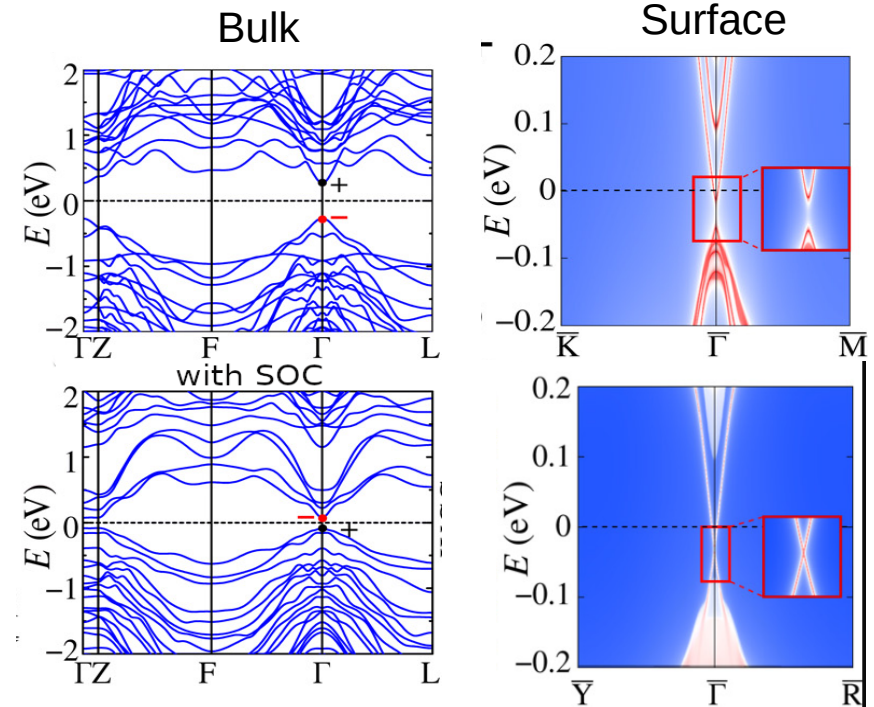# Interplay of topology and magnetic order

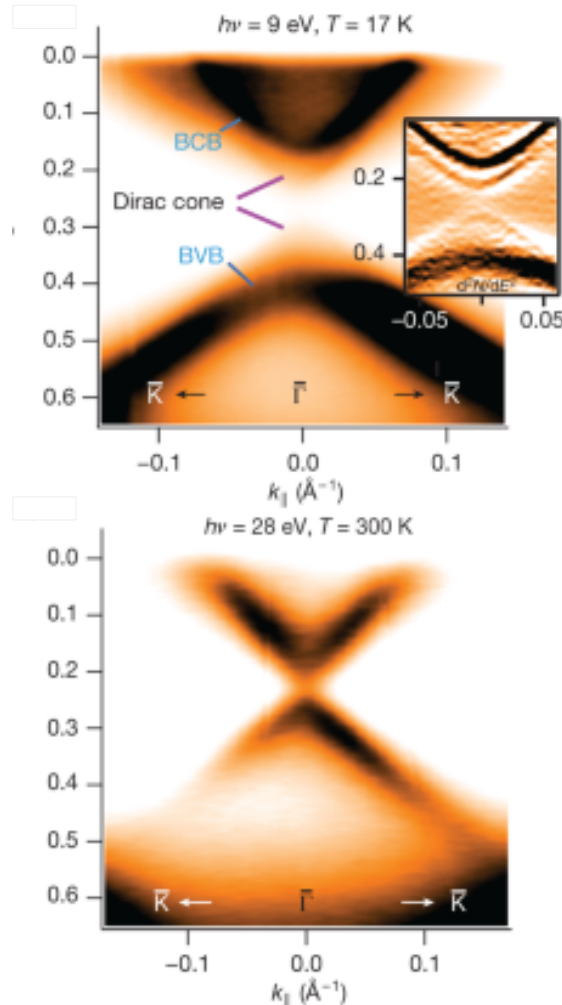## Topological Insulator
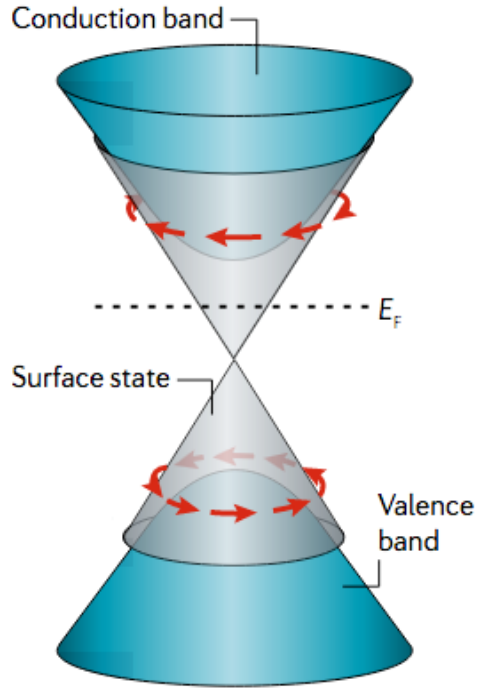
Magnetic topological Insulator

▸   Ordinarily realized by chemical doping of topological insulators with transition metal oxides

▸ **MnBi$_2$Te$_4$**: first intrinsic magnetic topological insulator predicted by DFT

Bulk

Surface

Tokura Y. et al,, Nature review Physics 1, 126-143 (2019)

J.Li et.al, Sci. Adv.5,eaaw5685(2019)

Experimental detection of magnetic gap in the surface states MnBi$_2$Te$_4$ films
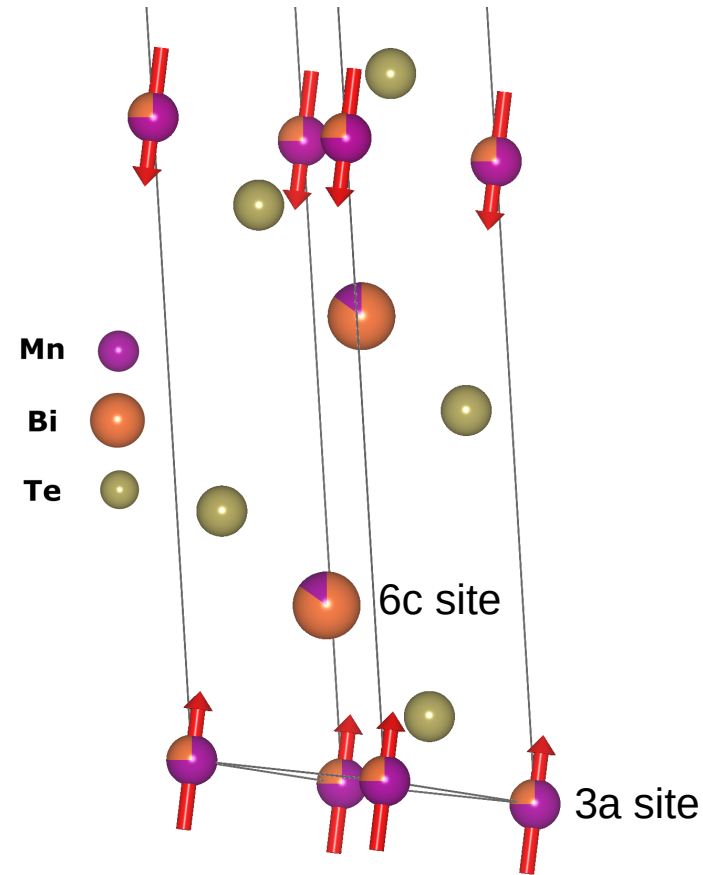

- ▸ The surface gap states are realized experimentally with ARPES and also STM measurements but under multiple tunning knobs including temperature, magnetic field, and pressure

- ▸ Highlights the fragility in the detection of the surface gap states

- ▸ Attributed from theoretical predictions to roles of antisite intermixing in the reduction of Dirac point gap
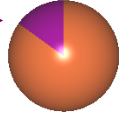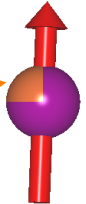
M.M Otrokov et al,, Nature 576, 416-422 (2019)

MnBi$_2$Te$_4$: highly tunable material platform


Mn
Bi
Te

Te   Bi
   Mn
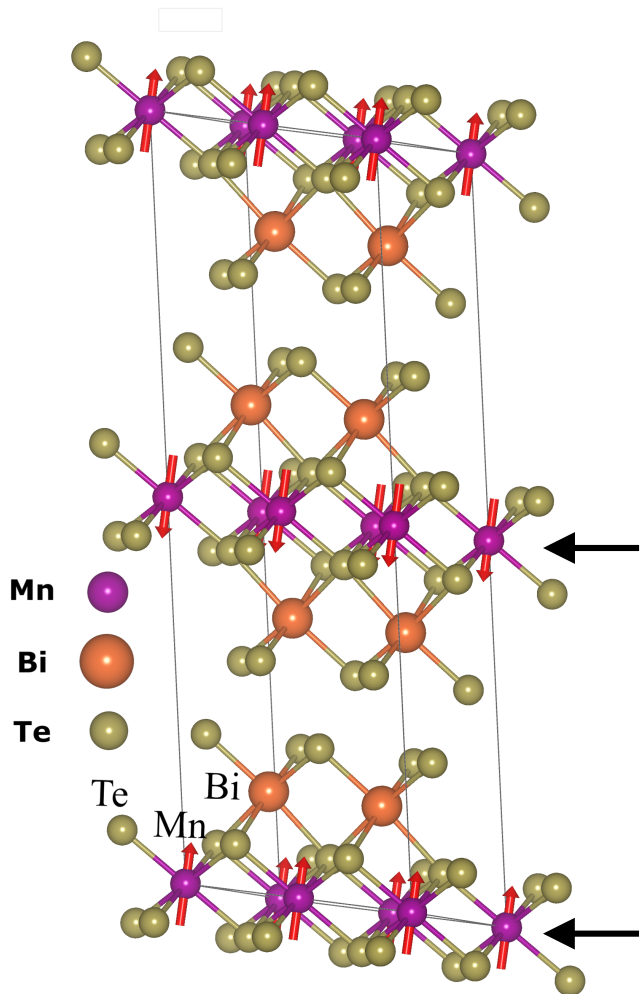
- ▸ Septuple layered Van der Waals compound

- ▸ Mn @ 3a (Mn$_{3a}$) & Bi @ 6c (Bi$_{6c}$) Wyckoff positions

- ▸ Local magnetic moments at the Mn$_{3a}$ sites adopt an A-type AFM order of FM alignment within the Mn layer.

- ▸ Aside the intrinsic properties, MnBi$_2$Te$_4$ is highly tunable

     Variations of chemical composition,

   – MnSb$_2$Te$_4$

   – MnBi$_2$Se$_4$

- ▸ Van der waals nature allows for interlacing the adjacent septuple layers with a number of of n nonmagnetic Bi$_2$Te$_3$ quintuple layers, thus the **(MnBi$_2$Te$_4$)(Bi$_2$Te$_3$)$_n$** family

J.Q Yan et al, Phys. Rev. Materials, 3, 064202 (2019)   Z.A Aliev et al,J. Alloys Compd., 789, 443-450 (2019)

Mn

Bi

Te

6c site

3a site

▸ Phase-pure polycrystalline samples

▸ Intermixing btw the Mn & pnictogen sites, whose composition depends on crystal growth conditions

▸ Mn dominates the 3a (Mn_{3a}) & Bi dominates the 6c site (Bi_{6c})

▸ with intermixing, Mn partially occupies (~0.006) the 6c site (Mn_{6c})

▸ while Bi partially occupies (0.22) the 3a site (Bi_{3a})

.

Mn

Bi

Te

6c site

3a site
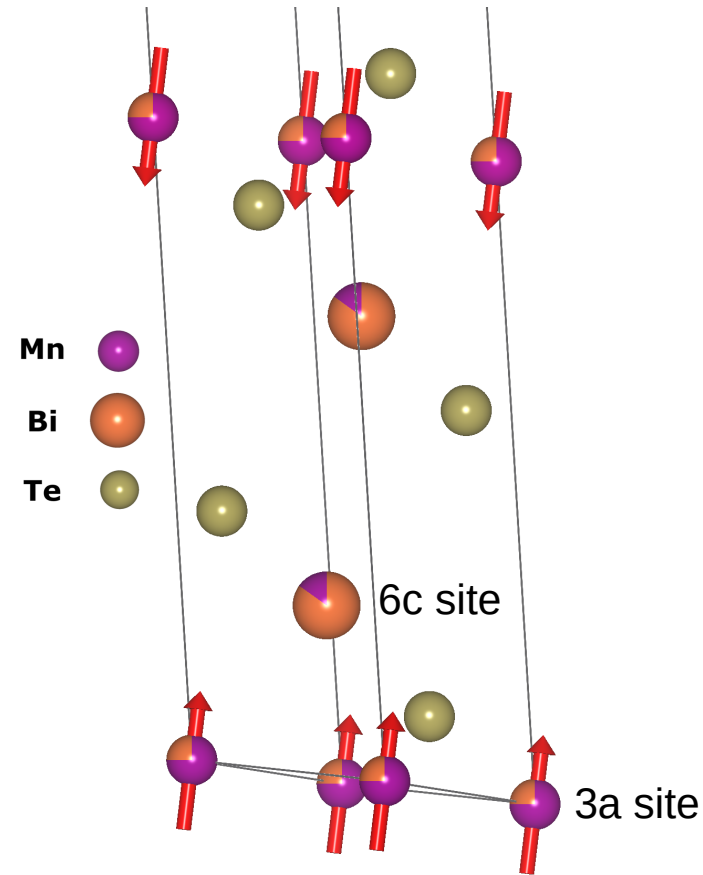
▸ Intersite-mixing is favoured by similar ionic radii e.g in $MnSb_2Te_4$, the Mn and Sn radii are closer.

▸ The strong intermixing in $MnSb_2Te_4$ promotes FM inter-layer coupling

▸ In $MnSb_2Te_4$, neutron diffraction measurements reveal local moment at the Mn_{6c} site and coupled antiferromagnetically to Mn_{3a}, i.e ferrimagnetic structure

▸ Instead for the **$(MnBi_2Te_4)(Bi_2Te_3)_n$** family, likely because of the lower levels of intermixing, neutron diffraction has been elusive so far on the roles and nature of antisites.
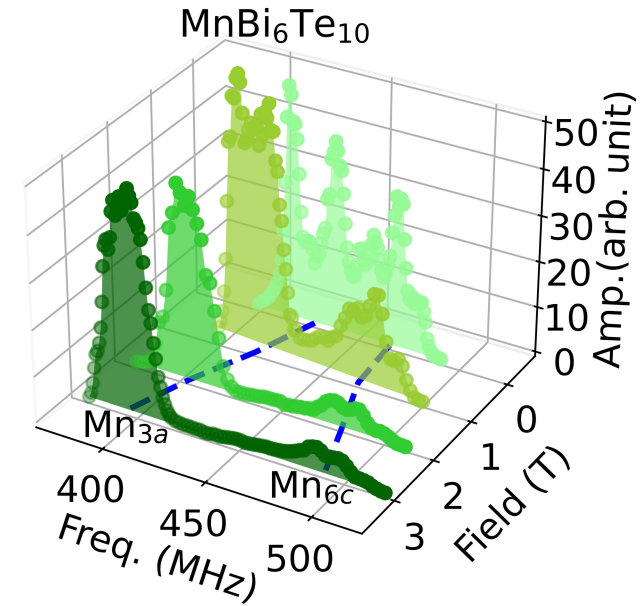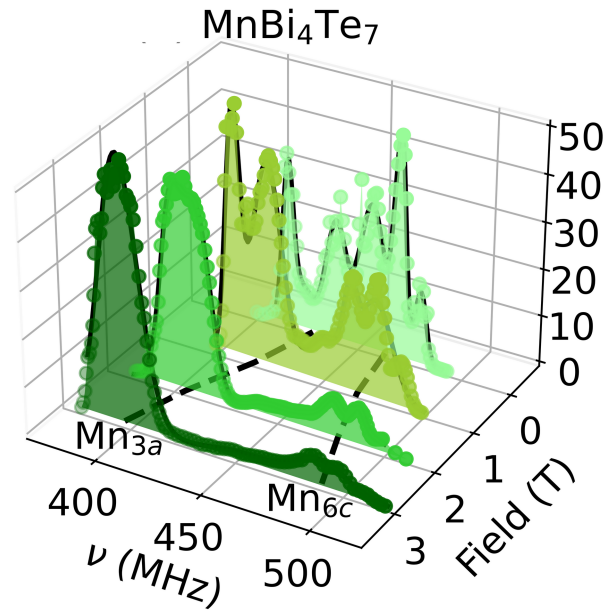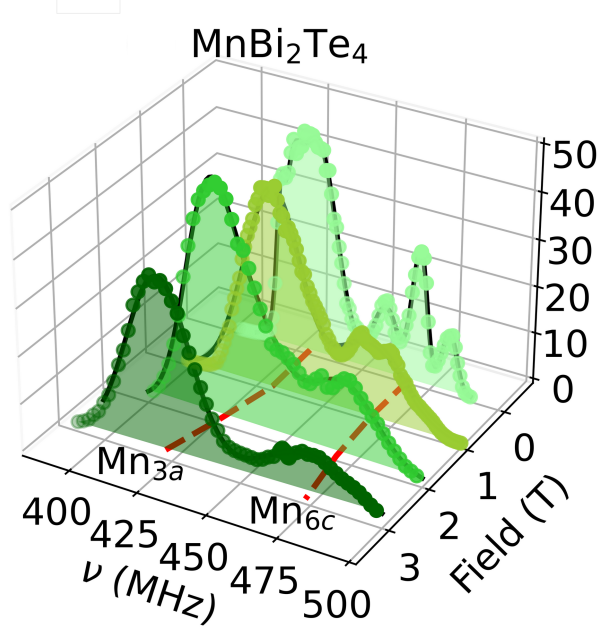
Y. Liu et al, Phys. Rev. X, 11, 021033 (2021), L Ding et al, PRB, 101, 020412(R) (2020)
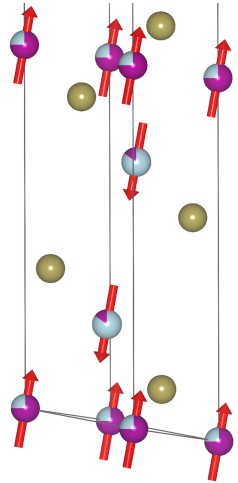
Investigate the nature of intermixing and its influence on the magnetic behaviour and phase diagram of the **$(MnBi_2Te_4)(Bi_2Te_3)_n$** family utilizing local probe techniques (NMR and μSR).
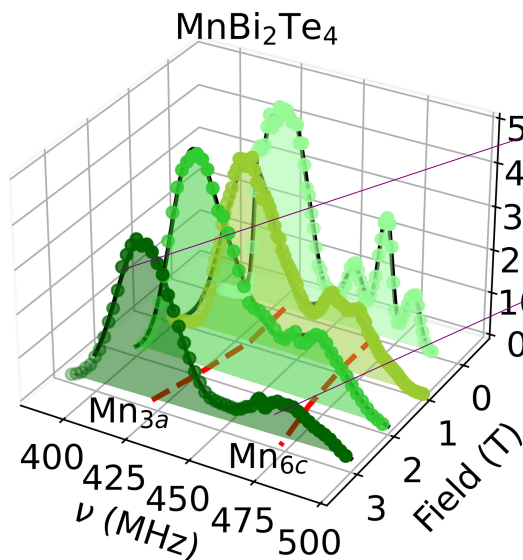
NMR results

^{55}Mn NMR peaks in the $(MnBi_2Te_4)(Bi_2Te_3)_n$ family

- NMR spectra at 1.4 K for increasing fields

- Two broad peaks pattern, with centers peaked at different frequencies

- Signifies two distinct ^{55}Mn sites, experiencing different local fields

- Frequency splits increases with the applied field

M. Sahoo, I. J. Onuorah *et al.*, *Adv. Sci.*, 11, 34, 2402753, 2024

^{55}Mn NMR peak assignment

MnBi$_2$Te$_4$
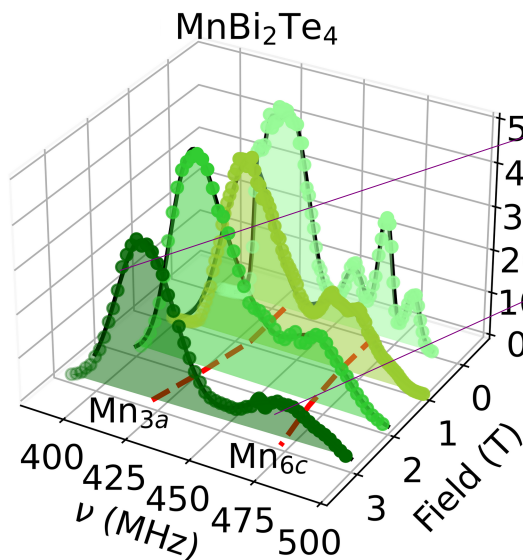
Mn$_{3a}$

Mn$_{6c}$

ν (MHz)

Field (T)

- ▸ At high fields (3T), enhancement more uniform,

- ▸ Considering large area, signal proportionality

- ▸ Mn$_{3a}$ lower frequency majority peaks

- ▸ Mn$_{6c}$ higher frequency minority peaks

$$^{55}\gamma(\mathcal{A} - 6\mathcal{B})g\mu_B S \ < \ ^{55}\gamma(\mathcal{A} - 6\textit{b})g\mu_B S$$

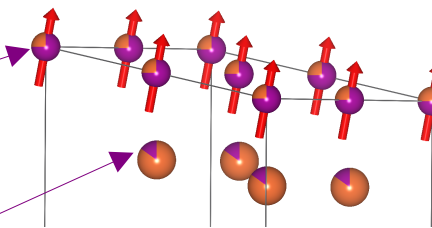Coupling from Mn$_{3a}$ n.n.

Coupling from Mn$_{6c}$ n.n.

M. Sahoo, I. J. Onuorah *et al.*, *Adv. Sci.*, 11, 34, 2402753, 2024

^{55}Mn NMR peak assignment

MnBi$_2$Te$_4$

ν (MHz): 400, 425, 450, 475, 500

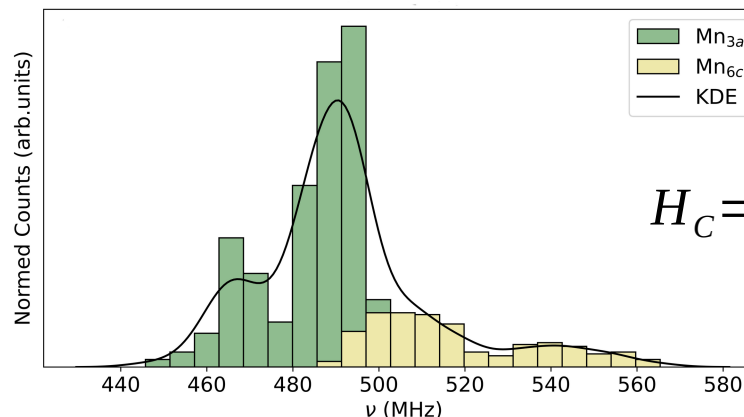Field (T): 0, 1, 2, 3

Mn$_{3a}$

Mn$_{6c}$

50 40 30 20 10 0

▸ At high fields (3T), enhancement more uniform,

▸ Considering large area, signal proportionality

▸ Mn$_{3a}$ lower frequency majority peaks

▸ Mn$_{6c}$ higher frequency minority peaks

▸ Confirmed with DFT calculated isotropic contact hyperfine at Mn$_{3a}$ & Mn$_{6c}$

$$^{55}\gamma(\mathcal{A} - 6\mathcal{B})g\mu_B\mathbf{S} < {}^{55}\gamma(\mathcal{A} - 6\mathcal{b})g\mu_B\mathbf{S}$$
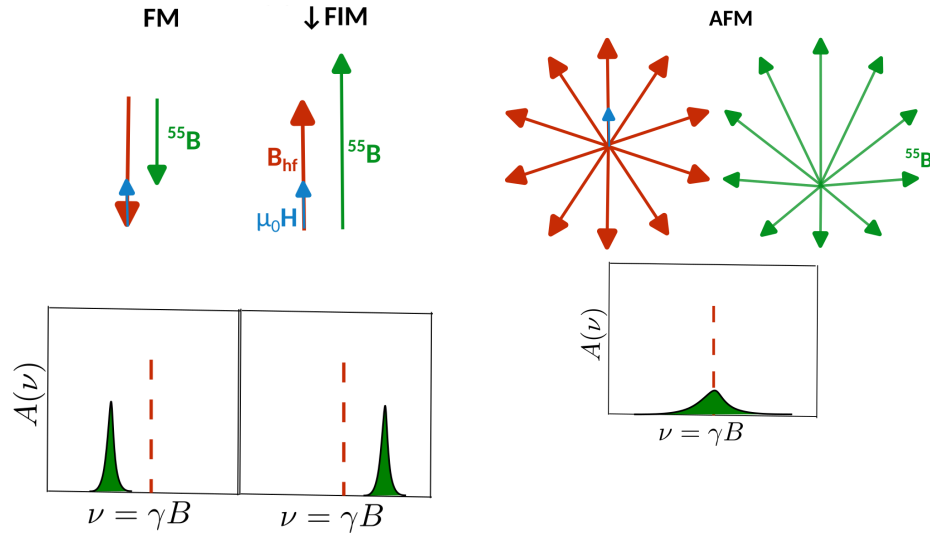
Coupling from Mn$_{3a}$ n.n.

Coupling from Mn$_{6c}$ n.n.

M. Sahoo, I. J. Onuorah *et al.*, *Adv. Sci.*, 11, 34, 2402753, 2024

Normed Counts (arb.units)

ν (MHz): 440, 460, 480, 500, 520, 540, 560, 580

Mn$_{3a}$
Mn$_{6c}$
KDE

$$H_C = \frac{\mu_0}{4\pi}\frac{8\pi}{3}\gamma_e\,\gamma_{jn}\,\delta(\boldsymbol{r_n})\,\boldsymbol{S}\cdot\boldsymbol{I_n}$$

^{55}Mn spin alignment assignment and magnetic order

▸ Orientation of moments at antisites from field vector composition $^{55}\mathbf{B} = \mu_o\mathbf{H} + \mathbf{B}_{hf}$
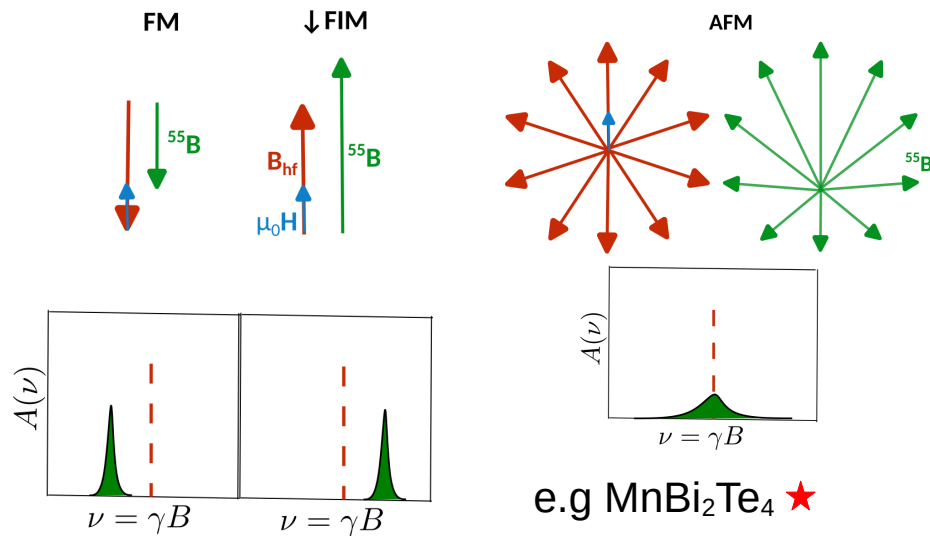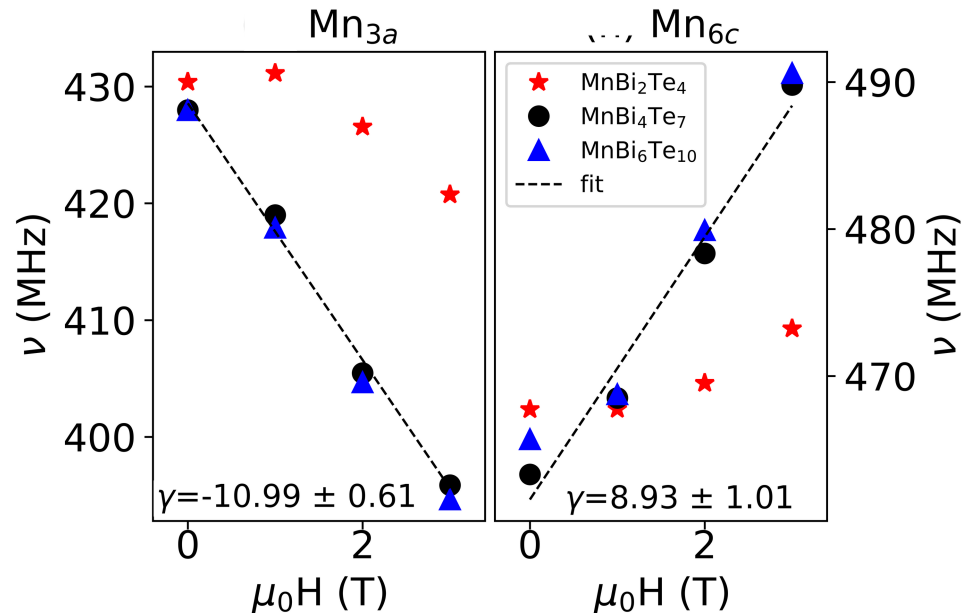
^{55}Mn spin alignment assignment and magnetic order

▸ Orientation of moments at antisites from field vector composition $^{55}\mathbf{B} = \mu_0\mathbf{H} + \mathbf{B}_{hf}$
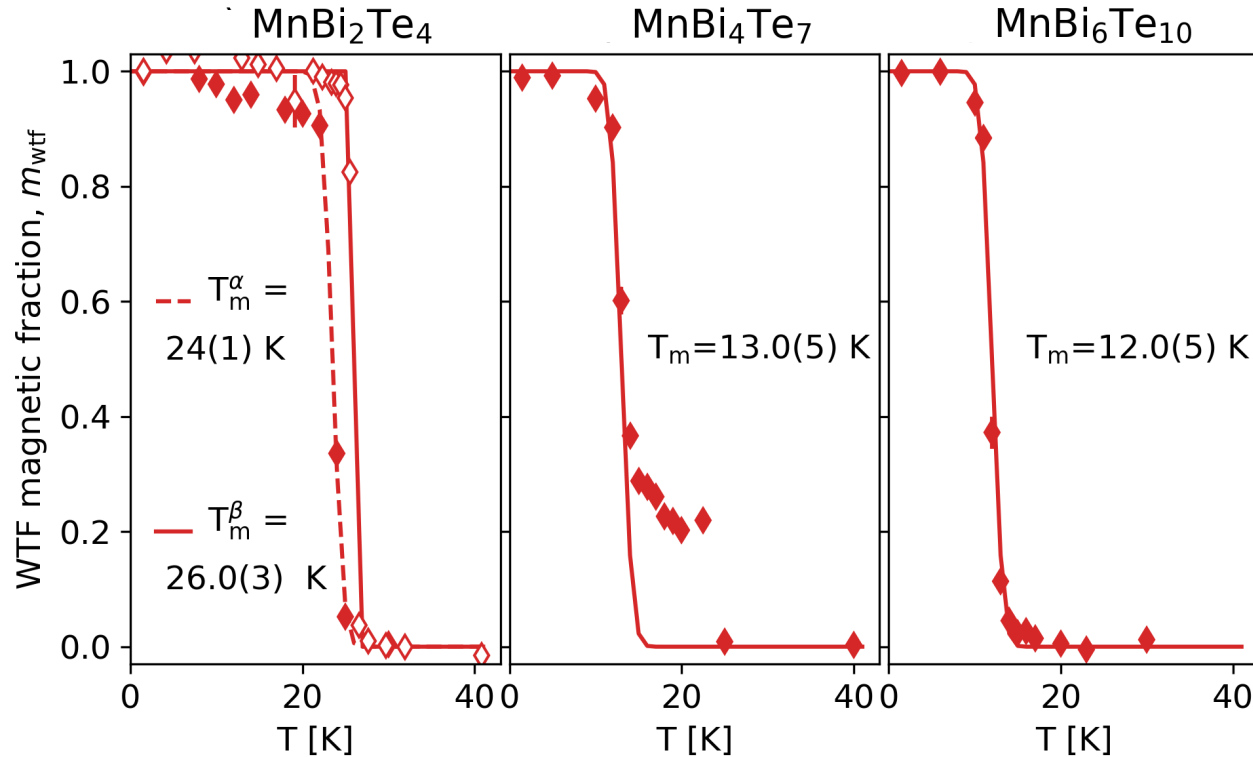

e.g MnBi$_2$Te$_4$ ★

e.g MnBi$_6$Te$_{10}$ ▲●

▸ Frequency shifts vs. applied field. Constant upto IT for MnBi$_2$Te$_4$ @Mn$_{3a}$ confirming AFM

▸ MnBi$_4$Te$_7$ and MnBi$_6$Te$_{10}$ follow the FM like vector composition

▸ Opposite slopes of the Mn$_{3a}$ and Mn$_{6c}$ shift line with field, indicate antiparallel spin alignment
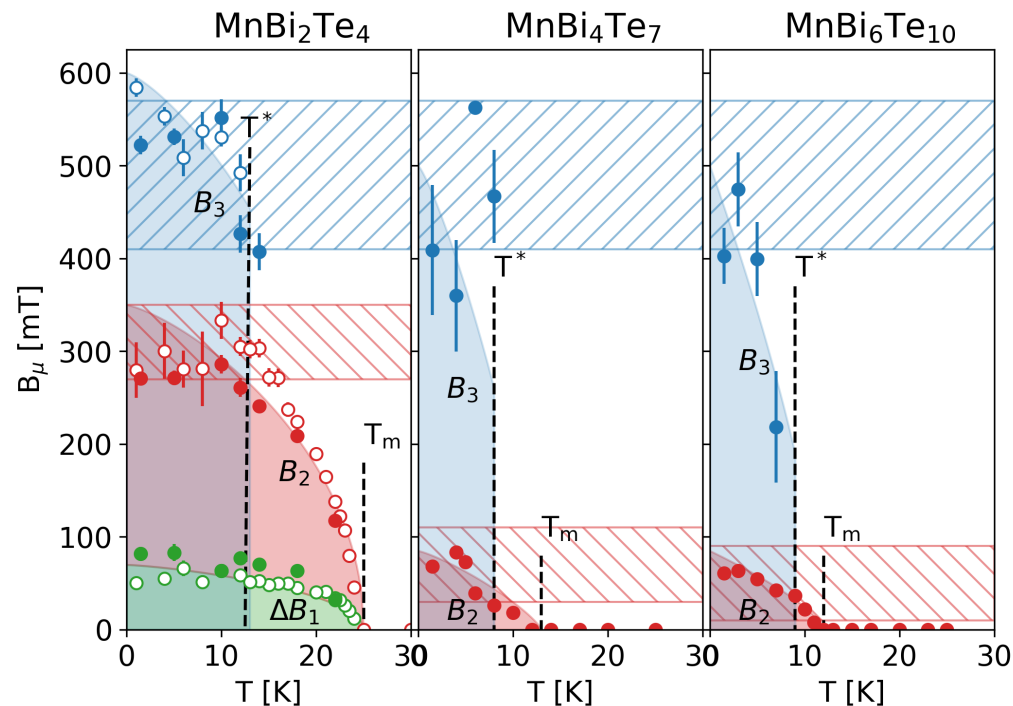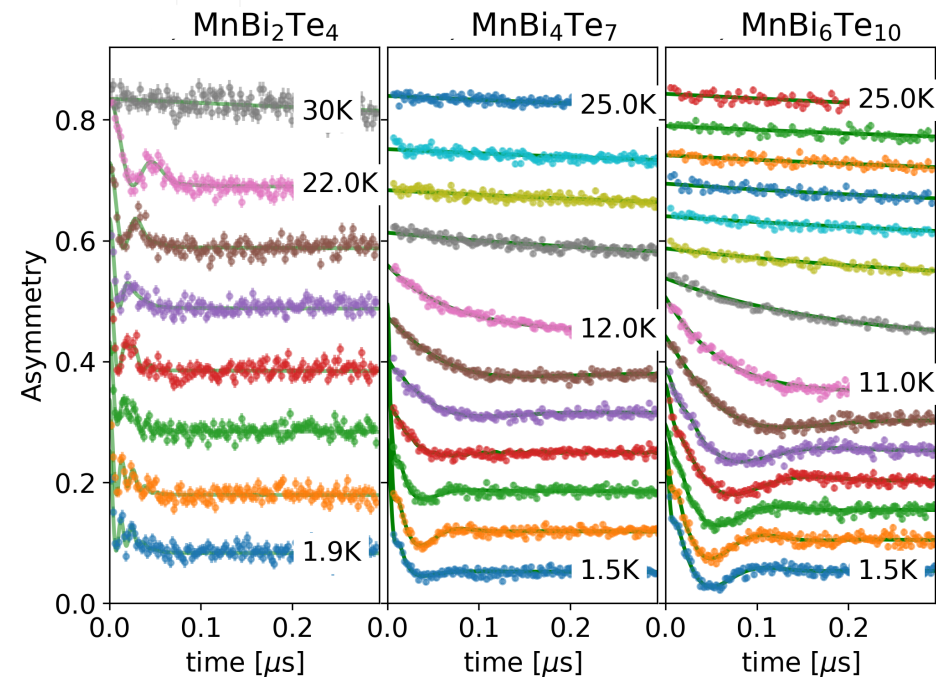
M. Sahoo, I. J. Onuorah *et al.*, *Adv. Sci.*, 11, 34, 2402753, 2024

µSR results

wTF-µSR

▸ Sharp transitions, despite atomic disorder

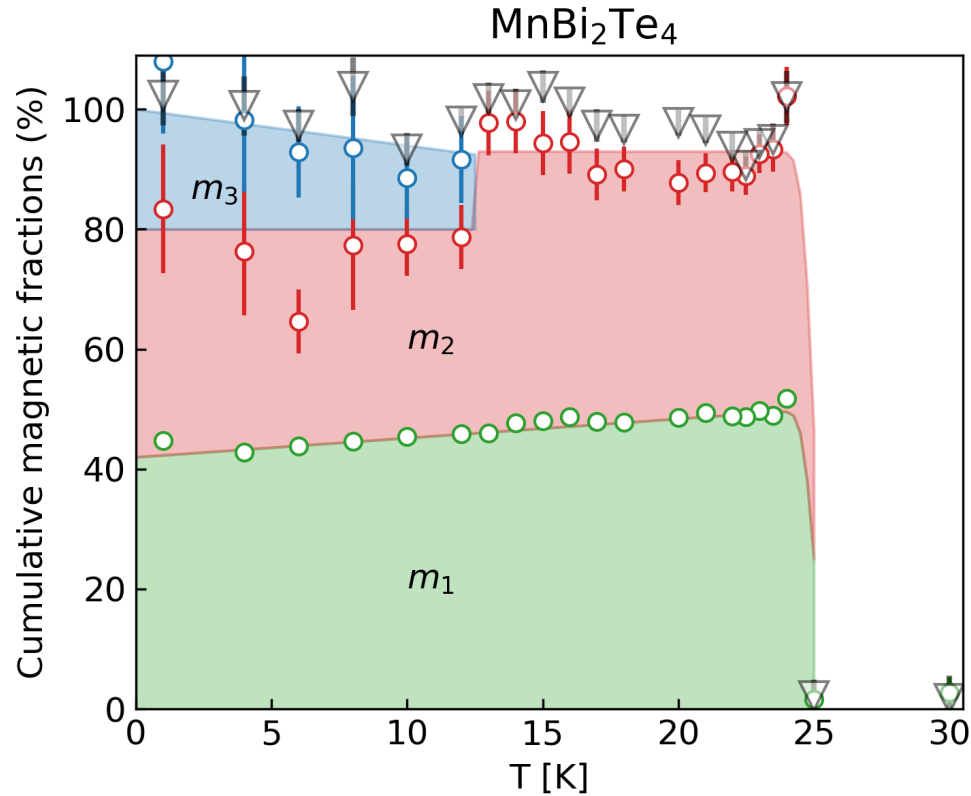M. Sahoo, I. J. Onuorah *et al.*, *Adv. Sci.*, 11, 34, 2402753, 2024

zF-μSR

- 2 damped field precessions + 1 fast initial decay: 3 broad field distributions. (n= 0 sample diff from n=1,2)

- The lower fields (ΔB_1 and B_2) vanish at the second-order magnetic transition T_m

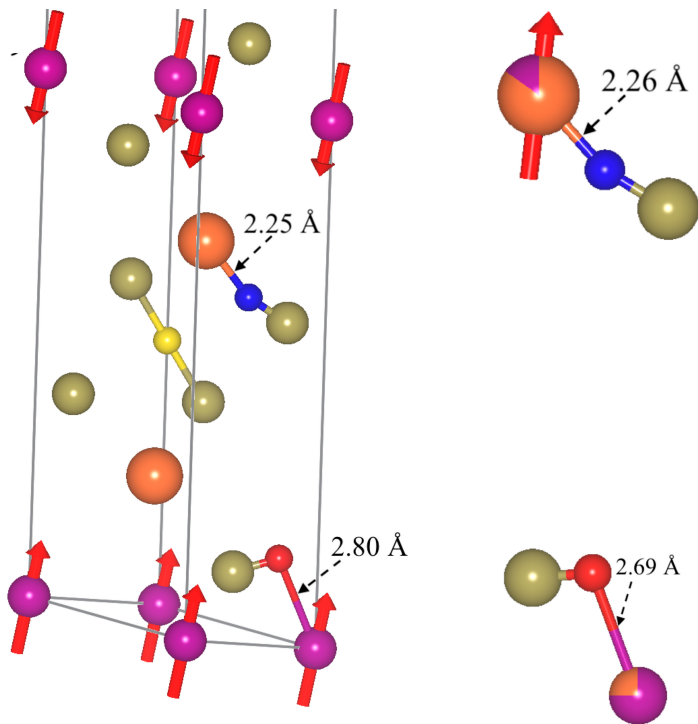- Large field disappears at an intermediate transition T* < T_m

ZF-µSR : Volume fraction and Cumulative magnetic fractions

MnBi$_2$Te$_4$

- ▸ m_L and $(m_1 + m_2)$ drop sharply at T_m

- ▸ m_3 disappears abruptly at T* → muon sites sensitive to the subtle change in the sample

M. Sahoo, I. J. Onuorah *et al.*, *Adv. Sci.*, 11, 34, 2402753, 2024

3 muon sites + 2 more B_μ with intermixing

2.26 Å

2.25 Å

2.80 Å

2.69 Å

$$B_\mu \approx B_{dip} + B_C + B_L$$

$$B_{dip} = \frac{\mu_0}{4\pi}\left(\frac{-\boldsymbol{m}}{r^3} + \frac{3(\boldsymbol{m}\cdot\boldsymbol{r})\boldsymbol{r}}{r^5}\right)$$

$$B_C = \frac{2\mu_0}{3}|\psi(0)|^2\boldsymbol{m}$$

M. Sahoo, I. J. Onuorah *et al.*, *Adv. Sci.*, 11, 34, 2402753, 2024

ZF-µSR – Muon sites and local field assignment with DFT+µ in $MnBi_2Te_4$

3 muon sites + 2 more B_μ with intermixing
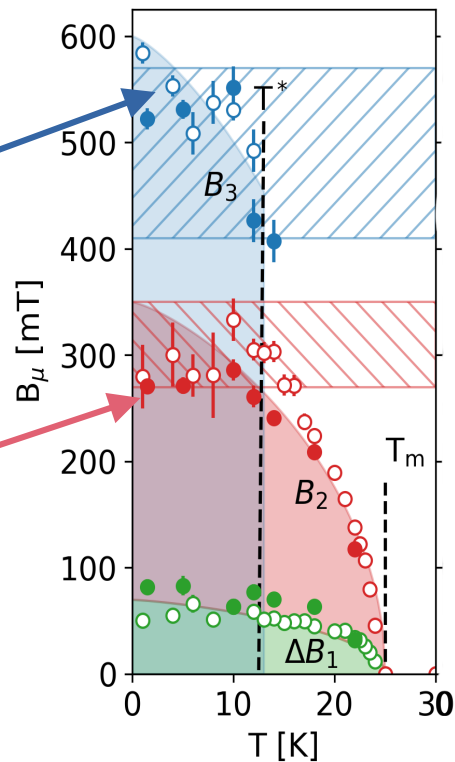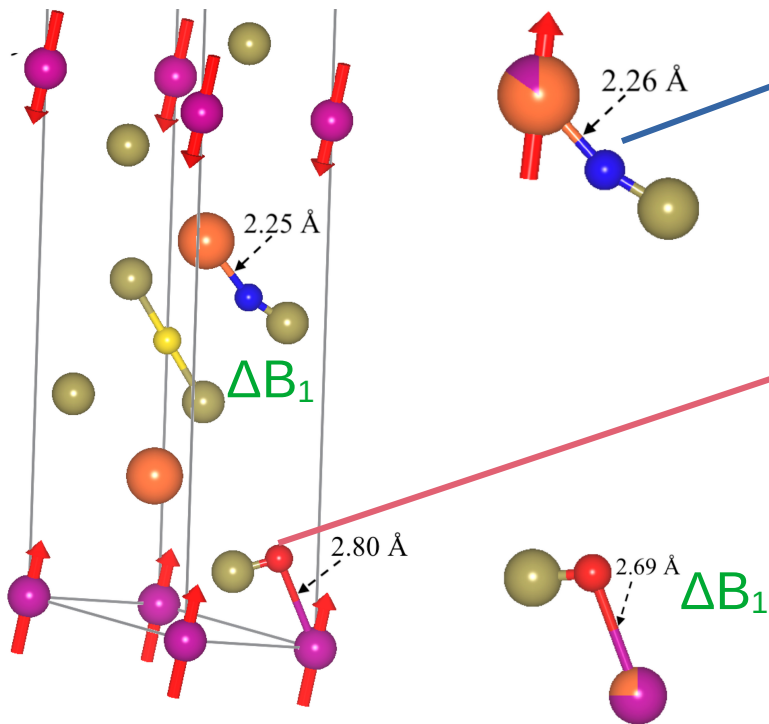
▸ Vanishing of B_3 at T* is due to the order-disorder of the magnetic moment at the antisite Mn_{6c}
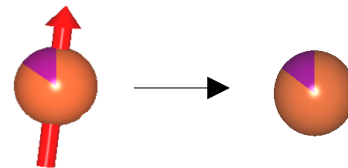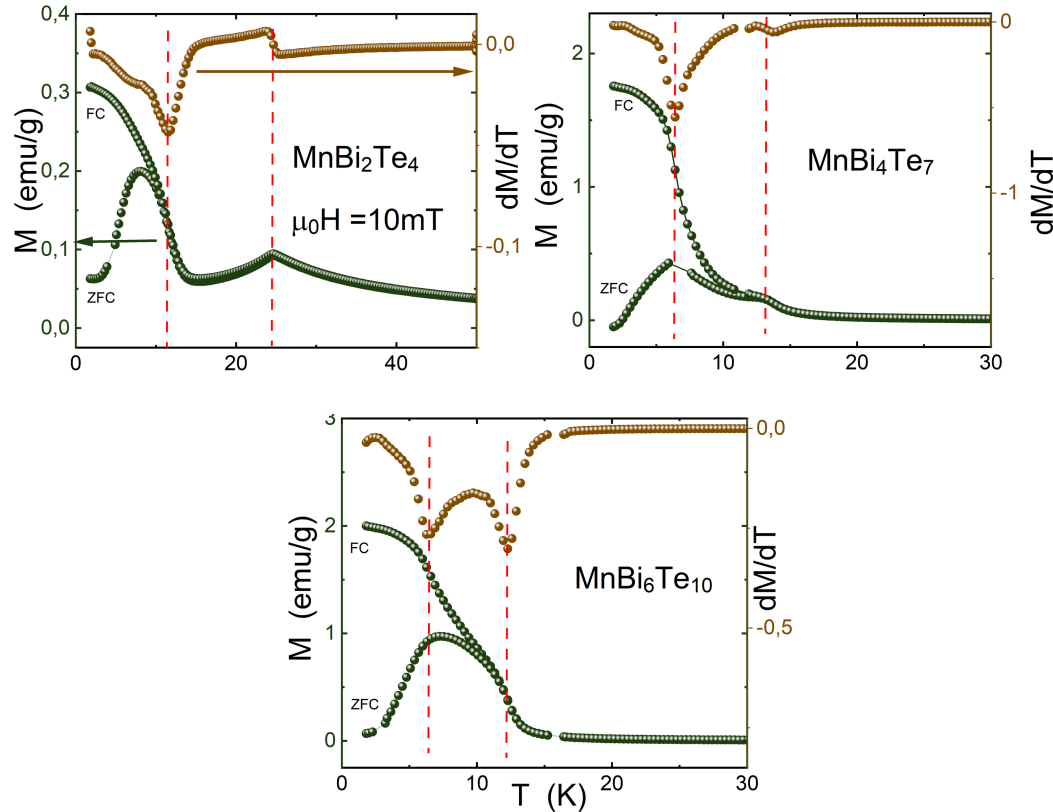

▸ No ΔB_1 in $MnBi_4Te_7$ and $MnBi_4Te_{10}$ but contribution from BL due to FM order → B_2

$$B_\mu \approx B_{dip} + B_C + B_L$$

$$B_{dip} = \frac{\mu_0}{4\pi}\left(\frac{-\boldsymbol{m}}{r^3} + \frac{3(\boldsymbol{m}\cdot\boldsymbol{r})\boldsymbol{r}}{r^5}\right)$$

$$B_C = \frac{2\mu_0}{3}|\psi(0)|^2 \boldsymbol{m}$$

Bulk Magnetic measurements

▸ The two transitions are observed for all the $(MnBi_2Te_4)(Bi_2Te_3)_n$ samples for the temperature dependence of the magnetization.

▸ Transition temperature values are consistent with µSR results

M. Sahoo, I. J. Onuorah *et al.*, *Adv. Sci.*, 11, 34, 2402753, 2024

Acknowledgment
Co-authors

Summary

▸ NMR results confirm site intermixing and reveal that the Mn magnetic moments of the native sites (Mn_{3a}) and the antisites (Mn6c) align opposite to each other in all the $(MnBi_2Te_4)(Bi_2Te_3)_n$.

▸ µSR results reveal two transitions in all the $(MnBi_2Te_4)(Bi_2Te_3)_n$ samples due to order-disorder of the Mn antisites magnetic moment.

▸ More attention is required in the specific temperature range T*<T<TN, where most magnetic Tis will most probably fulfill all theoretical predictions (large magnetic surface gap).